Search for electromagnetic properties of the neutrinos at the LHC

İ. Şahin*

Department of Physics, Zonguldak Karaelmas University, 67100 Zonguldak, Turkey

M. Köksal†

Department of Physics, Zonguldak Karaelmas University, 67100 Zonguldak, Turkey and

Department of Physics, Cumhuriyet University, 58140 Sivas, Turkey

Abstract

Exclusive production of neutrinos via photon-photon fusion provides an excellent opportunity to probe electromagnetic properties of the neutrinos at the LHC. We explore the potential of processes $pp \to p\gamma\gamma p \to p\nu\bar{\nu}p$ and $pp \to p\gamma\gamma p \to p\nu\bar{\nu}Zp$ to probe neutrino-photon and neutrino-two photon couplings. We show that these reactions provide more than seven orders of magnitude improvement in neutrino-two photon couplings compared to LEP limits.

*inancsahin@karaelmas.edu.tr

†mkoksal@cumhuriyet.edu.tr

I. INTRODUCTION

Neutrinos do not interact with photons in the standard model (SM). However, minimal extension of the SM with massive neutrinos yields neutrino-photon and neutrino-two photon interactions through radiative corrections [1–5]. Despite the fact that minimal extension of the SM induces very small couplings, there are several models beyond the SM predicting relatively large neutrino-photon and neutrino-two photon couplings. Electromagnetic properties of the neutrinos have important implications on particle physics, astrophysics and cosmology. Therefore probing electromagnetic structure of the neutrinos at colliders is important for understanding the physics beyond the SM and contributes to the studies in astrophysics and cosmology.

The Large Hadron Collider (LHC) generates high energetic proton-proton collisions with a high luminosity. It is commonly believed that it will help to answer many fundamental questions in particle physics. Recently a new phenomenon called exclusive production was observed in the measurements of CDF collaboration [6–12] and its physics potential has being studied at the LHC [13–27]. Complementary to proton-proton interactions, studies of exclusive production might be possible and opens new field of studying very high energy photon-photon and photon-proton interactions. Therefore it is interesting to investigate the potential of LHC as a photon collider to probe the electromagnetic properties of the neutrinos.

ATLAS and CMS collaborations have a program of forward physics with extra detectors located at distances of 220m and 420m from the interaction point [18, 21]. Range of these 220m and 420m detectors overlap and they can detect protons in a continuous range of ξ where ξ is the proton momentum fraction loss defined by the formula, $\xi = (|\vec{p}| - |\vec{p}\,'|)/|\vec{p}|$. Here $\vec{p}$ is the momentum of incoming proton and $\vec{p}\,'$ is the momentum of intact scattered proton. ATLAS Forward Physics (AFP) Collaboration proposed an acceptance of $0.0015 < \xi < 0.15$. There are also other scenarios with different acceptances of the forward detectors. CMS-TOTEM forward detector scenario spans $0.0015 < \xi < 0.5$ [16]. One of the well-known application of the forward detectors is the high energy photon-photon fusion. This reaction is produced by two quasireal photons emitted from protons. Since the emitted quasireal photons have a low virtuality they do not spoil the proton structure. Therefore scattered protons are intact and forward detector equipment allows us to detect intact scattered

protons after the collision.

The photon-photon fusion can be described by equivalent photon approximation (EPA) [14, 28, 29]. In the framework of EPA, emitted photons have a low virtuality and scattered with small angles from the beam pipe. Therefore they are almost real and the cross section for the complete process $pp \to p\gamma\gamma p \to pXp$ can be obtained by integrating the cross section for the subprocess $\gamma\gamma \to X$ over the effective photon luminosity $\frac{dL^{\gamma\gamma}}{dW}$

$$d\sigma = \int \frac{dL^{\gamma\gamma}}{dW}\, d\hat{\sigma}_{\gamma\gamma\to X}(W)\, dW \tag{1}$$

where W is the invariant mass of the two photon system and the effective photon luminosity is given by the formula

$$\frac{dL^{\gamma\gamma}}{dW} = \int_{Q^2_{1,min}}^{Q^2_{max}} dQ_1^2 \int_{Q^2_{2,min}}^{Q^2_{max}} dQ_2^2 \int_{y_{min}}^{y_{max}} dy \frac{W}{2y} f_1(\frac{W^2}{4y}, Q_1^2) f_2(y, Q_2^2) \tag{2}$$

with

$$y_{min} = \mathrm{MAX}(W^2/(4\xi_{max}E), \xi_{min}E), \;\; y_{max} = \xi_{max}E, \;\; Q^2_{max} = 2\mathrm{GeV}^2 \tag{3}$$

Here y is the energy of one of the emitted photons from the proton, f_1 and f_2 are the functions of the equivalent photon spectra. Equivalent photon spectrum of virtuality Q^2 and energy E_γ is given by

$$f = \frac{dN}{dE_\gamma dQ^2} = \frac{\alpha}{\pi}\frac{1}{E_\gamma Q^2}[(1 - \frac{E_\gamma}{E})(1 - \frac{Q^2_{min}}{Q^2})F_E + \frac{E_\gamma^2}{2E^2}F_M] \tag{4}$$

where

$$Q^2_{min} = \frac{m_p^2 E_\gamma^2}{E(E - E_\gamma)}, \;\; F_E = \frac{4m_p^2 G_E^2 + Q^2 G_M^2}{4m_p^2 + Q^2} \tag{5}$$

$$G_E^2 = \frac{G_M^2}{\mu_p^2} = (1 + \frac{Q^2}{Q_0^2})^{-4}, \quad F_M = G_M^2, \quad Q_0^2 = 0.71\mathrm{GeV}^2 \tag{6}$$

Here E is the energy of the incoming proton beam and m_p is the mass of the proton. The magnetic moment of the proton is taken to be $\mu_p^2 = 7.78$. F_E and F_M are functions of the electric and magnetic form factors. In the above EPA formula, electromagnetic form factors of the proton have been taken into consideration.

In this work we investigate the potential of exclusive $pp \to p\gamma\gamma p \to p\nu\bar{\nu}p$ and $pp \to p\gamma\gamma p \to p\nu\bar{\nu}Zp$ reactions at the LHC to probe $\nu\bar{\nu}\gamma$ and $\nu\bar{\nu}\gamma\gamma$ couplings. We obtain model independent bounds on these couplings considering Dirac neutrinos. During numerical analysis we assume that center of mass energy of the proton-proton system is $\sqrt{s} = 14$ TeV.

II. MODEL INDEPENDENT ANALYSIS

Non-standard $\nu\bar{\nu}\gamma$ interaction can be described by the following dimension 6 effective lagrangian [30–33]

$$\mathcal{L} = \frac{1}{2}\mu_{ij}\bar{\nu}_i\sigma_{\mu\nu}\nu_j F^{\mu\nu} \tag{7}$$

where μ_{ii} is the magnetic moment of ν_i and μ_{ij} $(i \neq j)$ is the transition magnetic moment. In the above effective lagrangian new physics energy scale Λ is absorbed in the definition of μ_{ii}. The most general dimension 7 effective lagrangian describing $\nu\bar{\nu}\gamma\gamma$ coupling is given by [5, 33–37]

$$\mathcal{L} = \frac{1}{4\Lambda^3}\bar{\nu}_i\left(\alpha^{ij}_{R1}P_R + \alpha^{ij}_{L1}P_L\right)\nu_j\tilde{F}_{\mu\nu}F^{\mu\nu} + \frac{1}{4\Lambda^3}\bar{\nu}_i\left(\alpha^{ij}_{R2}P_R + \alpha^{ij}_{L2}P_L\right)\nu_j F_{\mu\nu}F^{\mu\nu} \tag{8}$$

where $P_{L(R)} = \frac{1}{2}(1\mp\gamma_5)$, $\tilde{F}_{\mu\nu} = \frac{1}{2}\epsilon_{\mu\nu\alpha\beta}F^{\alpha\beta}$, α^{ij}_{Lk} and α^{ij}_{Rk} are dimensionless coupling constants.

Current experimental bounds on neutrino magnetic moment are stringent. The most sensitive bounds from neutrino-electron scattering experiments with reactor neutrinos are at the order of $10^{-11}\mu_B$ [38–41]. Bounds derived from solar neutrinos are at the same order of magnitude [42]. Bounds on magnetic moment can also be derived from energy loss of astrophysical objects. These give about an order of magnitude more restrictive bounds than reactor and solar neutrino probes [43–49]. Neutrino-two photon coupling has been less studied in the literature. Current experimental bounds on this coupling are derived from rare decay $Z \to \nu\bar{\nu}\gamma\gamma$ [33] and the analysis of $\nu_\mu N \to \nu_s N$ conversion [37]. LEP data on $Z \to \nu\bar{\nu}\gamma\gamma$ decay sets an upper bound of [33]

$$\left[\frac{1GeV}{\Lambda}\right]^6 \sum_{i,j,k}\left(|\alpha^{ij}_{Rk}|^2 + |\alpha^{ij}_{Lk}|^2\right) \leq 2.85 \times 10^{-9} \tag{9}$$

The analysis of the Primakoff effect on $\nu_\mu N \to \nu_s N$ conversion in the external Coulomb field of the nucleus N yields about two orders of magnitude more restrictive bound than $Z \to \nu\bar{\nu}\gamma\gamma$ decay [37].

In the presence of the effective interactions (7) and (8), $\gamma\gamma \to \nu\bar{\nu}$ scattering is described by three tree-level diagrams. The polarization summed amplitude square is given by the following simple formula

$$\langle |M|^2 \rangle = 4 \sum_{i,j,m,n} \mu_{im}\mu_{mj}\mu^*_{in}\mu^*_{nj} tu + \frac{s^3}{32\Lambda^6} \sum_{i,j,k} \left(|\alpha^{ij}_{Rk}|^2 + |\alpha^{ij}_{Lk}|^2 \right) \tag{10}$$

where s,t and u are the Mandelstam variables and we omit the mass of neutrinos. In the above amplitude we also neglect interference terms between interactions (7) and (8).

Neutrinos are not detected directly in the central detectors. Instead, their presence is inferred from missing energy signal. Therefore statistical analysis has to be performed with some care. Any SM process with final states which are not detected by the central detectors can not be discerned from $\gamma\gamma \to \nu\bar{\nu}$. ATLAS and CMS have central detectors with a pseudorapidity coverage $|\eta| < 2.5$. The SM processes with final state particles scattered with very large angles from the beam pipe may exceed the angular range of the central detectors. Hence any SM process with final states in the interval $|\eta| > 2.5$ should be accepted as a background for $\gamma\gamma \to \nu\bar{\nu}$. There are also other sources of backgrounds. The one which may affect our results is the instrumental background due to calorimeter noise. The calorimeter noise can be effectively suppressed by imposing a cut on the transverse energy of the jets. According to Ref.[50] the calorimeter noise is negligible for jets with a transverse energy greater than 40 GeV ($E_T > 40$ GeV). Of course the calorimeter noise is not the only factor which affects the jet efficiency. Based on [50] we take into account a global efficiency of 0.6. This is actually a prudent value for the global efficiency. We have considered the following background processes:

$$\begin{aligned} &\gamma\gamma \to \ell^-\ell^+; \quad \ell = e, \mu, \tau \\ &\gamma\gamma \to q\bar{q}; \qquad q = u, d, s, c, b \\ &\gamma\gamma \to W^+W^-; \quad W^\mp \to q\bar{q}', \ell\bar{\nu} \end{aligned} \tag{11}$$

Our backgrounds can be arranged into three classes:

(1)- $\gamma\gamma \to \ell^-\ell^+$, $\gamma\gamma \to q\bar{q}$ and $\gamma\gamma \to W^+W^- \to (q_1\bar{q}'_1, \bar{\ell}_1\nu_1)(q_2\bar{q}'_2, \ell_2\bar{\nu}_2)$ with $|\eta| > 2.5$ for all final charged particles.

(2)-$\gamma\gamma \to q\bar{q}$ and $\gamma\gamma \to W^+W^- \to (q_1\bar{q}'_1, \bar{\ell}_1\nu_1)(q_2\bar{q}'_2, \ell_2\bar{\nu}_2)$ with $|\eta| > 2.5$ for final charged leptons and $|\eta| < 2.5$, $E_T < 40$ GeV for final quarks, i.e., final quarks with $E_T < 40$ GeV are assumed to be missing even for $|\eta| < 2.5$.

(3)-We assume that 40% of the number of events from reactions $\gamma\gamma \to q\bar{q}$ and $\gamma\gamma \to W^+W^- \to (q_1\bar{q}_1', \bar{\ell}_1\nu_1)(q_2\bar{q}_2', \ell_2\bar{\nu}_2)$ with $|\eta| > 2.5$ for final charged leptons and $|\eta| < 2.5$, $E_T > 40$ GeV for final quarks is missing.

Among all the background processes the biggest contribution comes from electron-positron production with $|\eta| > 2.5$. The reason originates from the fact that the cross section is highly peaked in the forward and backward directions due to small mass of the electron and $t, u = 0$ pole structure. The sum of all background cross sections is $\sigma_{SM} = 27.24$ pb for $0.0015 < \xi < 0.5$ and $\sigma_{SM} = 26.80$ pb for $0.0015 < \xi < 0.15$.

We have estimated 95% confidence level (C.L.) bounds using one-parameter χ^2 test without a systematic error. SM prediction about missing number of events is $N_{SM} = 0.9 L_{int}\sigma_{SM}$. Here L_{int} is the integrated luminosity, 0.9 is the QED two-photon survival probability and σ_{SM} is the sum of all background cross sections. In order to test SM prediction we use the following χ^2 function:

$$\chi^2 = \left(\frac{\sigma_{\gamma\gamma\to\nu\bar{\nu}}}{\sigma_{SM}\ \delta_{stat}} \right)^2 \tag{12}$$

where $\sigma_{\gamma\gamma\to\nu\bar{\nu}}$ is the cross section for the process $\gamma\gamma \to \nu\bar{\nu}$ and $\delta_{stat} = \frac{1}{\sqrt{N_{SM}}}$ is the statistical error.

In tables I and II, we show 95% C.L. upper bounds of the couplings $\mu = \left(\sum_{i,j,m,n} \mu_{im}\mu_{mj}\mu^*_{in}\mu^*_{nj} \right)^{\frac{1}{4}}$ and $\alpha^2 = \sum_{i,j,k} \left(|\alpha^{ij}_{Rk}|^2 + |\alpha^{ij}_{Lk}|^2 \right)$. As we have mentioned, diagonal elements μ_{ii} are strictly constrained by the experiments. If we assume that μ_{ij} is diagonal then our limits are many orders of magnitude worse than the current experimental limits. On the other hand we see from the tables that our bounds on α^2 are approximately at the order of 10^{-16}. It is 7 orders of magnitude more restrictive than the LEP bound. As we have mentioned, during statistical analysis we consider the background processes given in (11). The main contribution is provided by the processes $\gamma\gamma \to e^-e^+, \mu^-\mu^+, u\bar{u}$ with $|\eta| > 2.5$. Of course there are other backgrounds that we have not taken into account. But these others are expected to give relatively small contributions. Furthermore, even a large background does not spoil our limits significantly. For instance, if we assume that background cross section is 4 times larger than the sum of all backgrounds that we have considered, our limits are spoiled only a factor of 2. They are still at the order of 10^{-16}.

The subprocess $\gamma\gamma \to \nu\bar{\nu}Z$ is described by 8 tree-level diagrams containing effective $\nu\bar{\nu}\gamma$ and $\nu\bar{\nu}\gamma\gamma$ couplings (Fig.1). The analytical expression for the amplitude square is

quite lengthy so we do not present it here. But it depends on the couplings of the form; $\sum_{i,j,k} |\alpha^{ij}_{Lk}|^2$, $\sum_{i,j,k} |\alpha^{ij}_{Rk}|^2$ and $\sum_{i,j,m,n} \mu_{im}\mu_{mj}\mu^*_{in}\mu^*_{nj}$ where we assume that $\mu_{kl} = \mu_{lk}$; $k, l = 1, 2, 3$. $\gamma\gamma \to \nu\bar{\nu}Z$ is absent in the SM at the tree-level. SM contribution is originated from loop diagrams involving 5 vertices. Since the SM contribution is very suppressed it is appropriate to set bounds on the couplings using a Poisson distribution. The expected number of events has been calculated considering the leptonic decay channel of the Z boson as the signal $N = 0.9 L_{int}\sigma BR(Z \to \ell\bar{\ell})$, where $\ell = e^-$ or μ^-. We also place a cut of $|\eta| < 2.5$ for final state e^- and μ^-. 95% C.L. upper bounds of the couplings $\alpha^2_L = \sum_{i,j,k} |\alpha^{ij}_{Lk}|^2$, $\alpha^2_R = \sum_{i,j,k} |\alpha^{ij}_{Rk}|^2$ and $\mu = \left(\sum_{i,j,m,n} \mu_{im}\mu_{mj}\mu^*_{in}\mu^*_{nj}\right)^{\frac{1}{4}}$ are presented in tables III and IV. We observe from the tables that the subprocess $\gamma\gamma \to \nu\bar{\nu}Z$ provides approximately an order of magnitude more restrictive bounds on $\nu\bar{\nu}\gamma\gamma$ coupling with respect to $\gamma\gamma \to \nu\bar{\nu}$. On the other hand both processes have almost same potential to probe the coupling μ.

III. CONCLUSIONS

Forward detector equipments allow us to study LHC as a high energy photon collider. By use of forward detectors we can detect intact scattered protons after the collision. Therefore deep inelastic scattering which spoils the proton structure, can be easily discerned from the exclusive photo-production processes. This provides us an opportunity to probe electromagnetic properties of the neutrinos in a very clean environment.

We show that exclusive $pp \to p\gamma\gamma p \to p\nu\bar{\nu}p$ and $pp \to p\gamma\gamma p \to p\nu\bar{\nu}Zp$ reactions at the LHC probe neutrino-two photon couplings with a far better sensitivity than the current limits. Former reaction improves the sensitivity limits by up to a factor of 10^7 and latter improves a factor of 10^8 with respect to LEP limits.

---

[1] B. W. Lee and R. E. Schrock, Phys. Rev. D **16**, 1444 (1977).

[2] W. Marciano and A. I. Sanda, Phys. Lett. B **67**, 303 (1977).

[3] B. W. Lynn, Phys. Rev. D **23**, 2151 (1981).

[4] R. J. Crewther, J. Finjord and P. Minkowski, Nucl. Phys. B **207**, 269 (1982).

[5] S. Dodelson and G. Feinberg, Phys. Rev. D **43**, 913 (1991).

[6] A. Abulencia *et al.* (CDF Collaboration), Phys. Rev. Lett. **98**, 112001 (2007).

[7] T. Aaltonen *et al.* (CDF Collaboration), Phys. Rev. Lett. **99**, 242002 (2007).

[8] T. Aaltonen *et al.* (CDF Collaboration), Phys. Rev. D **77**, 052004 (2008).

[9] T. Aaltonen *et al.* (CDF Collaboration), Phys. Rev. Lett. **102**, 242001 (2009).

[10] T. Aaltonen *et al.* (CDF Collaboration), Phys. Rev. Lett. **102**, 222002 (2009).

[11] O. Kepka and C. Royon, Phys. Rev. D **76**, 034012 (2007).

[12] M. Rangel, C. Royon, G. Alves, J. Barreto, and R. Peschanski, Nucl. Phys. B **774**, 53 (2007).

[13] S. M. Lietti, A. A. Natale, C. G. Roldao and R. Rosenfeld, Phys. Lett. B **497**, 243 (2001).

[14] K. Piotrzkowski, Phys. Rev. D **63**, 071502 (2001).

[15] V. A. Khoze, A. D. Martin, R. Orava and M. G. Ryskin, Eur. Phys. J. C **19**, 313 (2001).

[16] V. Avati and K. Osterberg, Report No. CERN-TOTEM-NOTE-2005-002, 2006.

[17] V. P. Goncalves and M. V. T. Machado, Phys. Rev. D **75**, 031502(R) (2007).

[18] C. Royon *et al.* (RP220 Collaboration), arXiv:0706.1796 [hep-ex].

[19] M. V. T. Machado, Phys. Rev. D **78**, 034016 (2008).

[20] O. Kepka and C. Royon Phys. Rev. D **78**, 073005 (2008).

[21] M.G. Albrow *et al.* (FP420 R and D Collaboration), JINST **4**, T10001 (2009), arXiv:0806.0302 [hep-ex].

[22] S. Atağ, S. C. İnan and İ. Şahin, Phys. Rev. D **80**, 075009 (2009), arXiv:0904.2687 [hep-ph].

[23] İ. Şahin and S. C. İnan, JHEP **09**, 069 (2009), arXiv:0907.3290 [hep-ph].

[24] S. Atağ, S. C. İnan and İ. Şahin, JHEP **09**, 042 (2010), arXiv:1005.4792 [hep-ph].

[25] S. C. İnan, Phys. Rev. D **81**, 115002 (2010), arXiv:1005.3432 [hep-ph].

[26] S. Atağ and A.A. Billur, arXiv:1005.2841 [hep-ph].

[27] M.G. Albrow, T.D. Coughlin and J.R. Forshaw, arXiv:1006.1289 [hep-ph].

[28] V. M. Budnev, I. F. Ginzburg, G. V. Meledin and V. G. Serbo, Phys. Rep. **15**, 181 (1975).

[29] G. Baur *et al.*, Phys. Rep. **364**, 359 (2002).

[30] F. Larios, R. Martinez and M. A. Perez, Phys. Lett. B **345**, 259 (1995).

[31] M. Maya *et al.*, Phys. Lett. B **434**, 354 (1998).

[32] N. F. Bell *et al.*, Phys. Rev. Lett. **95**, 151802 (2005).

[33] F. Larios, M. A. Perez and G. Tavares-Velasco, Phys. Lett. B **531**, 231 (2002).

[34] J. F. Nieves, Phys. Rev. D **28**, 1664 (1983).

[35] R. K. Ghosh, Phys. Rev. D **29**, 493 (1984).

[36] J. Liu, Phys. Rev. D **44**, 2879 (1991).

[37] S. N. Gninenko and N. V. Krasnikov, Phys. Lett. B **450**, 165 (1999).

[38] H. B. Li *et al.*, Phys. Rev. Lett. **90**, 131802 (2003).

[39] Z. Daraktchieva *et al.*, Phys. Lett. B **615**, 153 (2005).

[40] H. T. Wong *et al.*, Phys. Rev. D **75**, 012001 (2007).

[41] H. T. Wong *et al.*, Phys. Rev. Lett. **105**, 061801 (2010).

[42] C. Arpesella *et al.*, Phys. Rev. Lett. **101**, 091302 (2008).

[43] G. G. Raffelt, Phys. Rep. **320**, 319 (1999).

[44] V. Castellani and S. Degl'Innocenti, Astrophys. J. **402**, 574 (1993).

[45] M. Catelan, J. A. d. Pacheco and J. E. Horvath, Astrophys. J. **461**, 231 (1996) [arXiv:astro-ph/9509062].

[46] A. Ayala, J. C. D'Olivo and M. Torres, Phys. Rev. D **59**, 111901 (1999) [arXiv:hep-ph/9804230].

[47] R. Barbieri and R. N. Mohapatra, Phys. Rev. Lett. **61**, 27 (1988).

[48] J. M. Lattimer and J. Cooperstein, Phys. Rev. Lett. **61**, 23 (1988).

[49] A. Heger, A. Friedland, M. Giannotti and V. Cirigliano, Astrophys. J. **696**, 608 (2009) [arXiv:0809.4703 [astro-ph]].

[50] CMS Collaboration, *CMS Physics Technical Design Report Volume I*, Editor: D. Acosta, CERN/LHCC 2006-001.

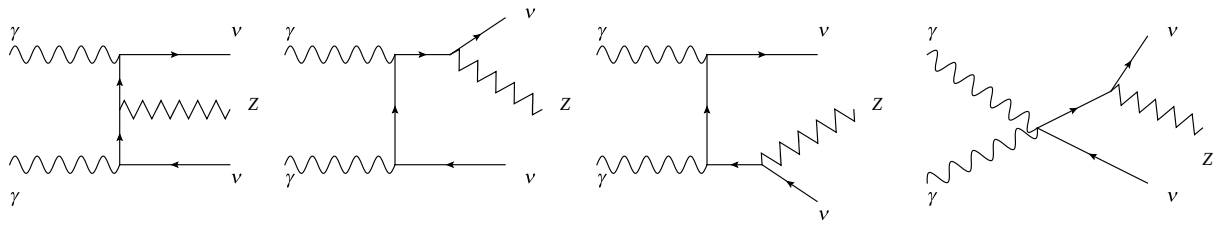

FIG. 1: Tree-level Feynman diagrams for the subprocess $\gamma\gamma \to \nu\bar{\nu}Z$. The crossed diagrams are not shown.

TABLE I: 95% C.L. upper bounds of the couplings μ and α^2 for the process $pp \to p\gamma\gamma p \to p\nu\bar{\nu}p$. We consider various values of the integrated LHC luminosities. Forward detector acceptance is $0.0015 < \xi < 0.5$. Λ is taken to be 1 GeV and limits of μ is given in units of Bohr magneton.

Luminosity:	$30fb^{-1}$	$50fb^{-1}$	$100fb^{-1}$	$200fb^{-1}$
μ	2.66×10^{-5}	2.50×10^{-5}	2.29×10^{-5}	2.10×10^{-5}
α^2	2.31×10^{-16}	1.79×10^{-16}	1.27×10^{-16}	8.96×10^{-17}

TABLE III: 95% C.L. upper bounds of the couplings μ and $\alpha^2_{L(R)}$ for the process $pp \to p\gamma\gamma p \to p\nu\bar{\nu}Zp$. We consider various values of the integrated LHC luminosities. Forward detector acceptance is $0.0015 < \xi < 0.5$. Λ is taken to be 1 GeV and limits of μ is given in units of Bohr magneton.

Luminosity:	$30fb^{-1}$	$50fb^{-1}$	$100fb^{-1}$	$200fb^{-1}$
μ	2.22×10^{-5}	1.95×10^{-5}	1.64×10^{-5}	1.38×10^{-5}
α^2_L	4.65×10^{-17}	2.79×10^{-17}	1.40×10^{-17}	6.98×10^{-18}
α^2_R	4.65×10^{-17}	2.79×10^{-17}	1.40×10^{-17}	6.98×10^{-18}

TABLE II: The same as table I but for $0.0015 < \xi < 0.15$.

Luminosity:	$30fb^{-1}$	$50fb^{-1}$	$100fb^{-1}$	$200fb^{-1}$
μ	3.11×10^{-5}	2.91×10^{-5}	2.67×10^{-5}	2.45×10^{-5}
α^2	1.79×10^{-15}	1.39×10^{-15}	9.82×10^{-16}	6.93×10^{-16}

TABLE IV: The same as table III but for $0.0015 < \xi < 0.15$.

Luminosity:	$30fb^{-1}$	$50fb^{-1}$	$100fb^{-1}$	$200fb^{-1}$
μ	3.64×10^{-5}	3.20×10^{-5}	2.70×10^{-5}	2.26×10^{-5}
α_L^2	2.43×10^{-15}	1.46×10^{-15}	7.30×10^{-16}	3.65×10^{-16}
α_R^2	2.43×10^{-15}	1.46×10^{-15}	7.30×10^{-16}	3.65×10^{-16}